# Dimensions of calcium release domains in frog skeletal muscle fibers

Julio L. Vergara[†], Marino DiFranco and David Novo

Department of Physiology, UCLA School of Medicine, Los Angeles, CA

## ABSTRACT

The spatiotemporal properties of the $Ca^{2+}$ release process in skeletal muscle fibers were determined using an improved confocal spot detection system. Muscle fibers were loaded with the low affinity fluorescent $Ca^{2+}$ indicator OGB-5N and localized action potential-induced fluorescence signals were recorded from consecutive locations separated by 200 nm within a single sarcomere. Three-dimensional reconstructions of the $Ca^{2+}$ transients illustrate the existence of domains of increased fluorescence around $Ca^{2+}$ release sites in the neighborhood of the T-tubules. We estimated the dimensions of these domains by drawing isochronal curves ($\Delta F/F$ vs. spot position) and fitting Gaussian profiles to them. It was found that the earliest detectable full-width-at-half-maximum of these profiles was 0.77 ± 0.25 μm and increased rapidly with time to 1.4 ± 0.2 μm at their peak (18 $^{o}$C). A brief, but statistically significant, delay of 0.8 ± 0.42 ms was observed between the onset of the fluorescence transients at the Z- and M-lines. Our results are compatible with the possibility that, in response to AP stimulation, $Ca^{2+}$ is not released exclusively from the junctional region of the sarcoplasmic reticulum, but from a broader expanse of the triadic region.

**Keywords:** Confocal spot detection, calcium transients, skeletal muscle, calcium domains, excitation-contraction coupling

## 1. INTRODUCTION

A critical step in the excitation-contraction (E-C) coupling process in skeletal muscle is the release of $Ca^{2+}$ ions, stored at a high concentration in the lumen of the terminal cisternae (TC) of the sarcoplasmic reticulum (SR), in response to electrical depolarization of the transverse tubular system (T-system)[1-3]. The structures supporting this release phase of E-C coupling are proposed to be the regions of the SR adjacent to the T-tubule, known as T-SR junctions, where $Ca^{2+}$ release channels (ryanodine receptor channels, RyR) and voltage sensors (dihydropyridine receptors, DHPRs) are presumed to be linked through protein-protein interactions[4-6]. Under physiological conditions, the electrical signal for $Ca^{2+}$ release in the muscle fiber is an action potential (AP) that spreads longitudinally through the sarcolemma and radially through the membranes of the T-system[7-10].

In frog skeletal muscle fibers, the T-SR junctions are remarkably well aligned with the Z-lines delimiting every sarcomere[1,4,11]; consequently, it is expected that in this preparation action potentials (APs) generate early increases in the $Ca^{2+}$ concentration ($[Ca^{2+}]$) at regions of the sarcomere close to the Z-line and smaller and more delayed changes at more remote regions (M-lines). The localization of the sites of $Ca^{2+}$ release to the Z-lines was first demonstrated experimentally by Escobar *et al.* (1994)[12] using a spot detection method and fluorescent $Ca^{2+}$ indicators. These authors observed that the AP-elicited $[Ca^{2+}]$ increase at the M-line was not significantly delayed relative to that at the Z-line (Z-M delay) and proposed that a broad band of the SR may participate in the release process[12]. However, this suggestion has remained questionable since limitations in the spatial resolution of the spot detection method could hinder the visualization of small Z-M delays[13-15]. Thus, the hypothesis that $Ca^{2+}$ release is localized to the T-SR junction hinges on the careful measurement of these delays and on whether they can be accounted for by passive $Ca^{2+}$ diffusion-reaction mechanisms in the sarcomere. Alternatively, $Ca^{2+}$ ions released from one region of the SR may lead to activation of the release of additional $Ca^{2+}$ from other regions of the SR through, for example, the positive feedback process known as Ca-induced-$Ca^{2+}$-release[16-18].

The goal of the experiments described here is to measure the spatiotemporal properties of the $[Ca^{2+}]$ changes that occur within a single sarcomere in a frog skeletal muscle fiber following AP stimulation, and to quantitatively assess the magnitude of Z-M delays. We utilized an enhanced spot detection methodology[12,19] in which the spatial resolution is that inherent to a confocal epifluorescence system[20,21].

[†] jvergara@mednet.ucla.edu; phone (310) 825-9307; fax (310) 206-3788; Department of Physiology, UCLA School of Medicine, 10833 LeConte Ave., 53-263 CHS, Los Angeles, CA 90095-1751

Biomarkers and Biological Spectral Imaging, Gregory H. Bearman, Darryl J. Bornhop, Richard M. Levenson, Editors, Proceedings of SPIE Vol. 4259 (2001)

## 2. METHODOLOGY

The general methodology and technical improvements of the confocal spot detection system utilized for the experiments presented below will be described extensively elsewhere[19]. We provide here a brief account of the major features of the confocal technique inasmuch as they are required to understand the experimental data.

### 2.1 Muscle fiber preparation and electrophysiological methods.

The experimental chamber and muscle fiber dissection and mounting procedures were as previously described[22]. Briefly, segments of cut single fibers from the dorsal head of the semitendinosus muscle from *Rana Catesbeiana* were mounted in an inverted double vaseline-gap chamber. The fibers were stretched to 3.7-4 μm to prevent contraction. Two vaseline seals isolated 3 segments of the fiber. The lateral segments were permeabilized with saponin (100 μg/ml; 1-3 min) to allow for free exchange between the lateral pool's solution and the intracellular milieu of the central segment of the fiber. The central pool was perfused with normal Ringer, whereas the lateral pools contained internal solution (see below). Experiments were performed between 17-21 $^{o}$C. APs were elicited by supra-threshold current pulses delivered to the muscle fiber through one lateral pool and recorded with a custom made electronic circuit[22]. The membrane potential at the central segment of the fiber was measured as the potential at the central pool minus the potential of lateral pool opposite to that used for current injection. APs were filtered at 10 kHz with an 8-pole Bessel filter (Frequency Devices, Haverhill, MA, USA) and digitized at 25-50 kHz using a PCI-MIO-16XE-10 data acquisition board (National Instruments, Austin, TX).

### 2.2 Solutions.

*Ringer's solution:* 114 mM NaCl; 2.5 mM KCl; 10 mM MOPS-Na; 1.8 mM $CaCl_2$, 10 mM dextrose. Isotonic high K: 110 mM $K_2SO_4$, 10 mM MOPS. *Internal solution:* 110 mM Aspartate-K; 20 mM MOPS-K; 1 mM $MgCl_2$, 5 mM $Na_2$-phosphocreatine, 5 mM $K_2$-ATP, 100-500 μM EGTA, 0.1 mg/ml Creatine-phosphokinase. The osmolality and pH of the solutions were adjusted to 250 mOsm/kg and 7.0, respectively.

### 2.3 Optical setup and stage scanning system.

The optical system was based on an inverted epifluorescence microscope (Model IM, Zeiss, Oberkochen, Germany). In addition to the standard bright-field configuration, it could operate as a stage scanning confocal or standard fluorescence microscope. In confocal mode, the 488 nm line of an Argon laser (Model 95, Lexel, Freemont, CA, USA) was focused onto a 5 μm pinhole (PH-5, Newport Corporation, Irvine, CA, USA). The pinhole image was projected using a 5x objective through the illumination port of the microscope. A 505DRLP dichroic mirror (Omega Optical, Brattleboro, VT, USA) directed the excitation light to a 100x high NA oil immersion objective (Plan Fluor 100, 1.3 NA, Nikon, Japan) that focused it to a 0.6 μm spot on the preparation. The fluorescence image of the illumination spot was collected with the same lens, passed through a 515 nm long pass emission filter (Omega Optical) and centered on a 50 μm pinhole (04PIP013, Melles Griot, Rochester, NY, USA) used to mask the square active area (200 μm per side) of a PIN photodiode (HR008, United Detector Technology, Hawthorne, CA, USA), which served as the light detector. The photocurrent was amplified using an integrating patch-clamp unit (Axopatch 200B, Axon Instruments, Foster City, CA) and filtered at 2-5 kHz using an 8-pole Bessel filter (Frequency Devices). The optical signal and the AP were acquired simultaneously using the acquisition board described above. A shutter (22510A1S5, Vincent and Associates, Rochester, NY) was used to control the illumination time of the sample.

The experimental chamber and the electronic headstage were mounted on a custom-made microscope stage. Two open-loop motorized drives (860A-2, Newport) were used for coarse movement of the stage in the x- or y-direction (orthogonal to the optical axis of the microscope). In addition, a high-resolution nanotranslator (Model TSE-150, Burleigh Instruments, Inc., Fishers, New York), driven by an inchworm motor with a closed loop integral linear encoder, permitted positioning of the stage along the x-axis with 50 nm resolution. A 6000ULN controller (Burleigh Instruments) was used to drive the inchworm motor under computer control using custom-written software in G-language (Labview, National Instruments). This software was also used to control a stepper motor (Z-Axis1, Prairie Technologies, Waunakee, WI) driving the focusing mechanism of the microscope (z-axis) with 500 nm resolution. In stage scanning confocal mode, the specimen was moved in the x direction while the confocal spot remained stationary and the long axis of the muscle fiber was aligned parallel to the x-axis of the microscope stage. The lateral (x-y) and axial (z) resolution of the confocal system was determined *in vitro* using 0.1-2.0 μm (diameter) fluorescently labeled latex beads (Fluorospheres, size kit #2, Molecular Probes, Eugene, OR). The beads were attached to a glass coverslip and bathed in water or embedded in 40% glucose, 0.5% agarose in order to mimic the refractive index of the fiber[15,23]. Beads were scanned in the x- and z-directions in 100 and 500 nm steps, respectively. Plots of fluorescence vs. the spot position were fit to Gaussian functions and their full-width-at-half-maximum (FWHM) was used as evaluate the width of the intensity profile. For comparison, the plots of fluorescence of beads of different diameters were normalized to their maxima.

**2.4 Measurement and analysis of $Ca^{2+}$-dependent fluorescence transients.**

The salt form of the $Ca^{2+}$ indicator Oregon Green 488 BAPTA-5N (OGB-5N) (Molecular Probes) was added at 200-500 μM concentrations to the cut ends and allowed to diffuse into the muscle fiber 45-60 minutes prior to optical measurements being started. Figure 1 illustrates the typical experimental protocol used to acquire localized fluorescence transients in response to a single AP stimulation of the muscle fiber. Figure 1, *traces a* and *b* correspond to simultaneously acquired records of the AP and the OGB-5N fluorescence, respectively. Approximately 20 ms after starting the acquisition, and 60 ms before the stimulation of the fiber, the laser shutter was opened to acquire the baseline fluorescence ($F_{rest}$, *trace b)*. The AP elicited a rapid increase in fluorescence to a peak $\Delta F_{peak}$, which was followed by a decay to baseline within ~40 ms. *Trace c* of Figure 1 defines relevant parameters that will be used to define the kinetic features of the $Ca^{2+}$ transient, expressed in terms of $\Delta F/F$[24,25]. The amplitude of the transient was characterized by its $(\Delta F/F)_{peak}$ value and its specific duration by the full-duration-at-half-maximum (FDHM). The delay time ($t_d$) corresponds to the period between the time of stimulus delivery (t = 0) and the initiation of the rising phase of the transient, defined as the first moment when the fluorescence is sustained for 1 ms at 3 standard deviations (SD's) above $F_{rest}$. The rising phase of the transient was characterized by the rise time (*rt*), defined as interval between the initiation and the peak of the transient. All the kinetic parameters were calculated directly from the sampled data by a custom-made computer program written in Delphi (Borland, Scotts Valley, CA, USA).

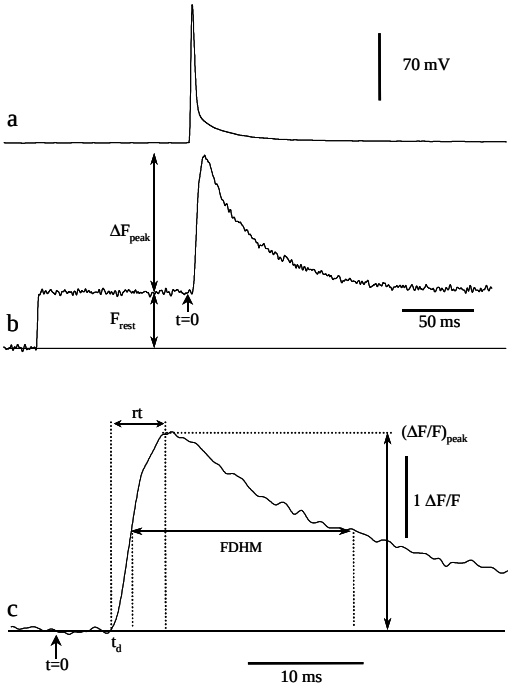


*Figure 1. Confocal detection of fluorescence transients*. The action potential (*trace a*) and the $Ca^{2+}$-dependent OGB-5N fluorescence changes (*trace b*) were simultaneously recorded when the detection spot was placed at a Z-line. The resting potential and the amplitude of the AP are 100 and 145 mV, respectively. The characteristic parameters of the fluorescence transient (*trace c*) are: $t_d$ = 5 ms; *rt* = 4.8 ms; $(\Delta F/F)_{peak}$ = 2.5; FDHM = 21 ms. Experimental conditions: [EGTA]: 100 μM; [OGB-5N]: 500 μM; temperature: 17°C; sarcomere spacing: 4.3 μm.

To determine the spatial dependence of $[Ca^{2+}]$ changes, the illumination spot was initially focused in the z-axis to within 10 μm from the bottom coverslip and on a random location with respect to the fiber's sarcomere structure. Subsequently, individual fluorescent transients elicited by AP stimulation were recorded every 5-10 s from adjacent sites, separated by 100-200 nm, along the x-axis. The combination of stretching and the use of exogenous intracellular $Ca^{2+}$ buffers (OGB-5N and EGTA) prevented any fiber movement, as evidenced by direct observation under the microscope and the lack of movement artifacts in the optical records.

To estimate the free $[Ca^{2+}]$ underlying fluorescence transients, we used a deconvolution formula (based on an equilibrium approximation[25]) that requires independent measurements of the maximum and minimum fluorescence of the indicator ($F_{max}$ and $F_{min}$, respectively). $F_{max}$ was measured *in vivo* at the end of the experiment, as previously described[25]. $F_{min}$ was assumed to correspond to the resting fluorescence of the fiber since OGB-5N is a $Ca^{2+}$ indicator with very low affinity ($K_d$ = 32 μM[26]) and the average resting $[Ca^{2+}]$ of amphibian muscle fibers is ~100 nM[27].

**2.5 T-tubule staining and sarcomere length measurements.**

In order to correlate the positional-dependence of the $Ca^{2+}$ transients with specific structures of the sarcomere, the muscle fibers were stained with the non-permeant fluorescent potentiometric dye di-8-ANEPPS (Molecular Probes), which specifically labels the T-system[10,28]. Experiments involving di-8-ANEPPS were performed using either dual- or single-staining protocols. In the dual staining experiments, the fibers were intracellularly stained with OGB-5N and subsequently externally stained with di-8-ANEPPS (1-10 μg/ml in Ringer) for ~30 minutes. Confocal spot measurements were performed as described above in order to localize the $Ca^{2+}$-dependent fluorescence transients with respect to the T-tubule fluorescence. In single staining experiments, the fiber was externally perfused for ~30 minutes with 1-10 μg/ml di-8-ANEPPS in Ringer solution prior to mounting in the experimental chamber. The fiber was scanned with the confocal spot in 100 or 200 nm steps

and the fluorescence was acquired at every position. Since in these measurements the source of fluorescence (the T-tubule) represents a sub-resolution object[10,29,30], in principle it can be used to test the optical resolution of our microscope *in vivo*.

## 3. RESULTS

### 3.1 Evaluation of the spatial resolution of the confocal spot system.

To determine the lateral resolution of our spot detection system, we scanned beads of known sizes along the x-axis and determined the FWHM of their intensity profiles. Two examples of these scans are shown in Figure 2A for beads of 0.2 and 1.0 μm in diameter. It can be observed that the Gaussian fits to the data points for each bead are readily distinguishable, as reflected by the significantly different FWHM values of 0.27 and 0.99 μm, respectively. The relationship between FWHM and bead diameter is shown in Figure 2B for a wide range of bead sizes. From this plot it can be deduced that the FWHM provides an accurate experimental measurement of the actual diameter for beads ranging in size between 0.5 and 2.0 μm, as illustrated by the close match between the linear regression and the equality line. However, the FWHM of beads smaller than 0.5 μm deviates from linearity and asymptotically approaches the limit of resolution of the optical system. It should be noted that, although 0.2 and 0.1 μm beads could not be distinguished from each other, they still appeared significantly smaller than 0.5 μm beads ($p<0.005$). Thus, the FWHM of 0.3 μm obtained with these very small beads represents the minimum fluorescence object that we can resolve, thus defining the lateral (x-axis) resolution of the microscope. A similar trend, but with a much more severe limitation in the resolution, was observed with the same size beads scanned in the z-direction (data not shown). In this case we determined[19] that the axial (z-axis) resolution is ~0.75 μm, a result that is in good agreement with fluorescence confocal theory for a 1.3 NA objective[20,31].

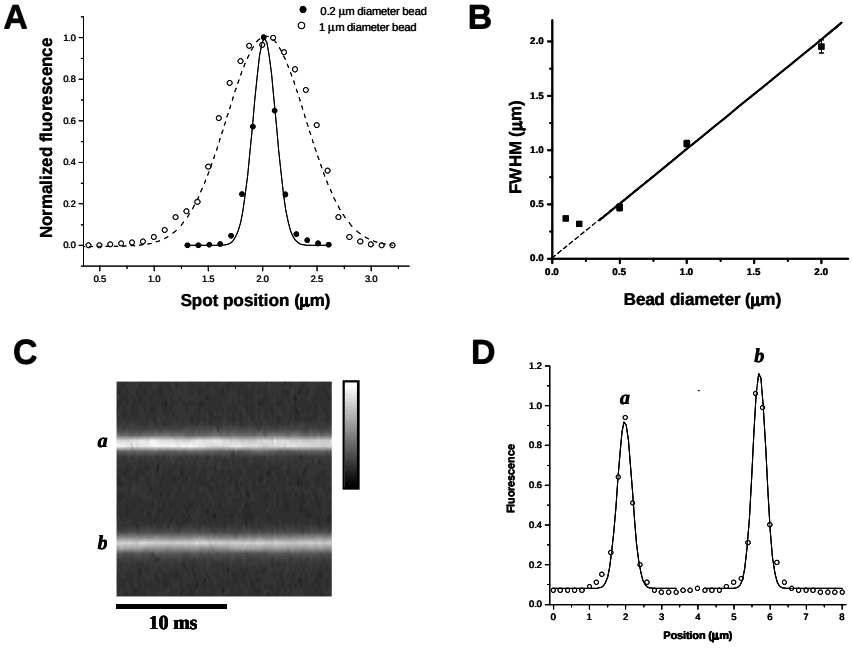


*Figure 2: Assessment of the spatial resolution of the confocal system.* **A:** Normalized fluorescence data obtained from x-axis scans of calibration beads. Closed and open circles represent data from 0.2 and 1.0 mm beads, respectively. Solid and dashed lines represent their respective Gaussian fits, with FWHM of 0.27 and 0.99 μm, respectively. **B:** Comparison of actual bead diameter to FWHM determined from the x-axis scans of several beads of 0.1 (n = 5), 0.2 (n = 16), 0.5 (n = 16), 1.0 (n = 6) and 2.0 (n = 5) μm in diameter. The solid line is a linear regression fit (slope = 1.01, intercept = $5x10^{-4}$ and r = 0.995) for the 0.5, 1.0 and 2.0 mm beads. The dashed line represents the equality $y = x$. **C:** Grayscale image of the T-tubule fluorescence built from traces acquired from 40 adjacent confocal spot positions in a fiber stained with di-8-ANEPPS. The acquisition time was 20 ms per trace, and the records were taken at positions separated by 200 nm. The direction of scan is vertical and time is horizontal. The calibration bar represents 50 grayscale levels, corresponding to fluorescence values from 0 to 1.2, and has a length of 4 μm. **D:** Time average of the fluorescence intensity in every record used to make up the image in C, plotted as a function of the spot position. The solid lines are Gaussian fits to the fluorescence data, yielding a FWHM of 0.48 and 0.44 μm, for peaks *a* and *b* respectively.

We measured the lateral dimension of T-tubules from fibers stained with di-8-ANEPPS[10,28], under the same conditions in which $Ca^{2+}$ detection experiments are performed (see below), and verified if it was close to values obtained in vitro for very small beads. Figure 2C is an image constructed from typical stage-scan fluorescence traces, which depicts the fluorescence intensity (in grayscale levels) as a function of time and spot position. The total distance scanned was 8 μm, corresponding to approximately two sarcomeres. The negligible fluorescence observed in the space between two adjacent T-tubules demonstrates that there is no apparent misregistration of sarcomeres above and below the focal plane of the illumination/detection spot. This is further documented in Figure 2D, which corresponds to a time-average fluorescence

profile of the scans in Figure 2C. In this figure, the T-tubules appear as very narrow peaks of fluorescence whose spatial distribution can be readily evaluated quantitatively by fitting to Gaussian functions. It can be seen that the background fluorescence is very low and the ratio between the peak fluorescence intensity and the baseline is ~10. Gaussian fits of pooled data from experiments like that shown in Figures 2C and 2D, yield a mean T-tubule FWHM of 0.49 ± 0.08 (Mean ± SD, n = 15).

### 3.2 Location dependence of OGB-5N fluorescence transients.

Figure 3A shows a family of fluorescence transients obtained by scanning a fiber stained intracellularly with OGB-5N. The length of the scan spanned half a sarcomere from the Z-line (trace 1) to the M-line (trace 11). In agreement with previous reports[12,15], transients recorded at the Z-line are significantly faster and larger than those recorded at the M-line. The electrical trace shown in Figure 3A is the superposition of the 11 APs that elicited the fluorescence transients. They are identical to within 1 mV, thus excluding variations on the electrical properties of the muscle fiber as a possible cause for the positional dependent variance in the evoked fluorescence transients. As illustrated in Figures 3A, the kinetic features of the transients recorded at intermediate locations between the M- and Z-line vary continuously from their extreme values at these positions. The rising phase of the evoked transients becomes slower (*rt* increases from 5.1 to 13.2 ms) as the recording position moves from the Z- to the M-line. It should be noted that the falling phases of the transients do not cross each other and there is no evidence of secondary release processes following the peak. The onset of the fluorescent transients at the M-line, seen in Figure 3A, is delayed by <0.7 ms with respect to the Z-line. Data pooled from 36 experiments performed under similar conditions (the [EGTA] was 0.5 mM instead of 0.1 mM and the temperature was 18°C) revealed that the mean Z-M delay, calculated as the average of the differences in $t_d$ between Z- and M-line ΔF/F transients, is only 0.86 ± 0.42 ms. This is a surprisingly small number since, if we consider that the average distance between the Z- and M-lines is ~2 μm, it would imply an average rate of spread of $Ca^{2+}$ along the sarcomere of ~2.3 μm/ms. Finally, the large difference in $(\Delta F/F)_{peak}$ between the Z- and the M-line fluorescence transients (2.5 vs. 0.8, respectively) demonstrates the existence of large intrasarcomeric $Ca^{2+}$ gradients. After ~30 ms these gradients collapse, as evidenced by the fact that the transients fuse together at this time.

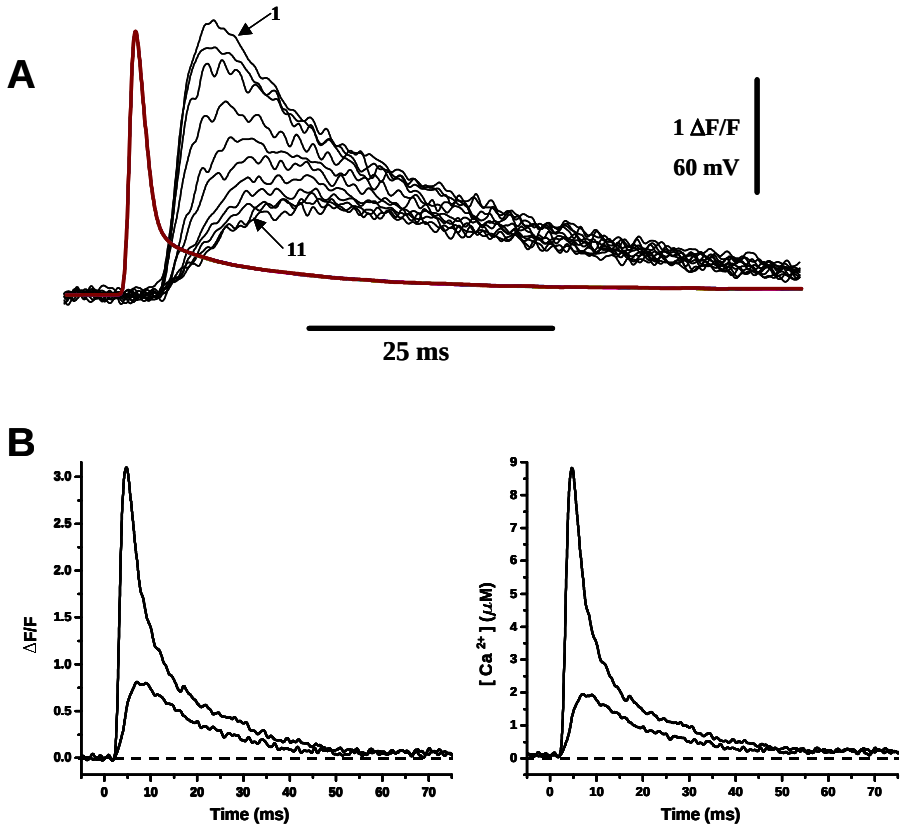


*Figure 3. Positional dependence of fluorescence and [$Ca^{2+}$] transients detected form a single sarcomere in fiber perfused internally with 500 μM OGB-5N.* **A**: Superimposed OGB-5N ΔF/F transients (1 through 11) and APs recorded at 10 adjacent spot positions every 200 nm along a line parallel to the fiber axis. Traces 1 and 11 correspond to transients recorded at the Z-line and M-line, respectively. The APs are a superimposition of the 11 APs that evoked the fluorescence transients. Temperature: 17°C; sarcomere spacing: 4.3 μm; [EGTA]: 0.1 mM. **B:** *Left panel*, fluorescence transients (ΔF/F) recorded at the Z- and M-lines from another fiber. *Right panel*, [$Ca^{2+}$] traces calculated using the calibration procedures described in Methods and assuming a [$Ca^{2+}$] baseline of 100 nM. The dashed lines represent the zero level for both plots. Temperature: 19.2°C, sarcomere spacing: 4 μm; [EGTA]: 0.5 mM.

In order to estimate the magnitude of the [$Ca^{2+}$] changes underlying localized fluorescence transients, we performed the calibration procedures described in Methods. Figure 3B shows a comparison between ΔF/F transients recorded at the Z- and M-line (left panel) and their corresponding deconvoluted [$Ca^{2+}$] transients (right panel). The peak [$Ca^{2+}$] was 8.8 μM for the Z-line and 2 μM for the M-line. With the caveat that, within the detection spot, OGB-5N is at equilibrium throughout the time course of the transients, the apparent similarity in kinetics between [$Ca^{2+}$] and ΔF/F transients indicates that the changes in [$Ca^{2+}$] were constrained to the linear range of the $Ca^{2+}$-dye saturation curve[26]. This is reinforced by the similarity of the ratio between $(\Delta F/F)_{peak}$ at Z- and M-lines (3.9) and that between peak [$Ca^{2+}$] values (4.5). The [$Ca^{2+}$] transients shown in Figure 3B were calculated using a ratio between $F_{max}$ and $F_{rest}$ of 15, which is similar to the average value obtained in other 4 saturation experiments (15 ± 1, n = 5).

### 3.3 Dimensions of AP-evoked fluorescence domains.

The concept of a $Ca^{2+}$ domain, a localized increase in [$Ca^{2+}$] as a function of space and time, has been introduced to characterize $Ca^{2+}$-entry sites in excitable cells[32,33]. The experimental determination of the properties of AP-evoked

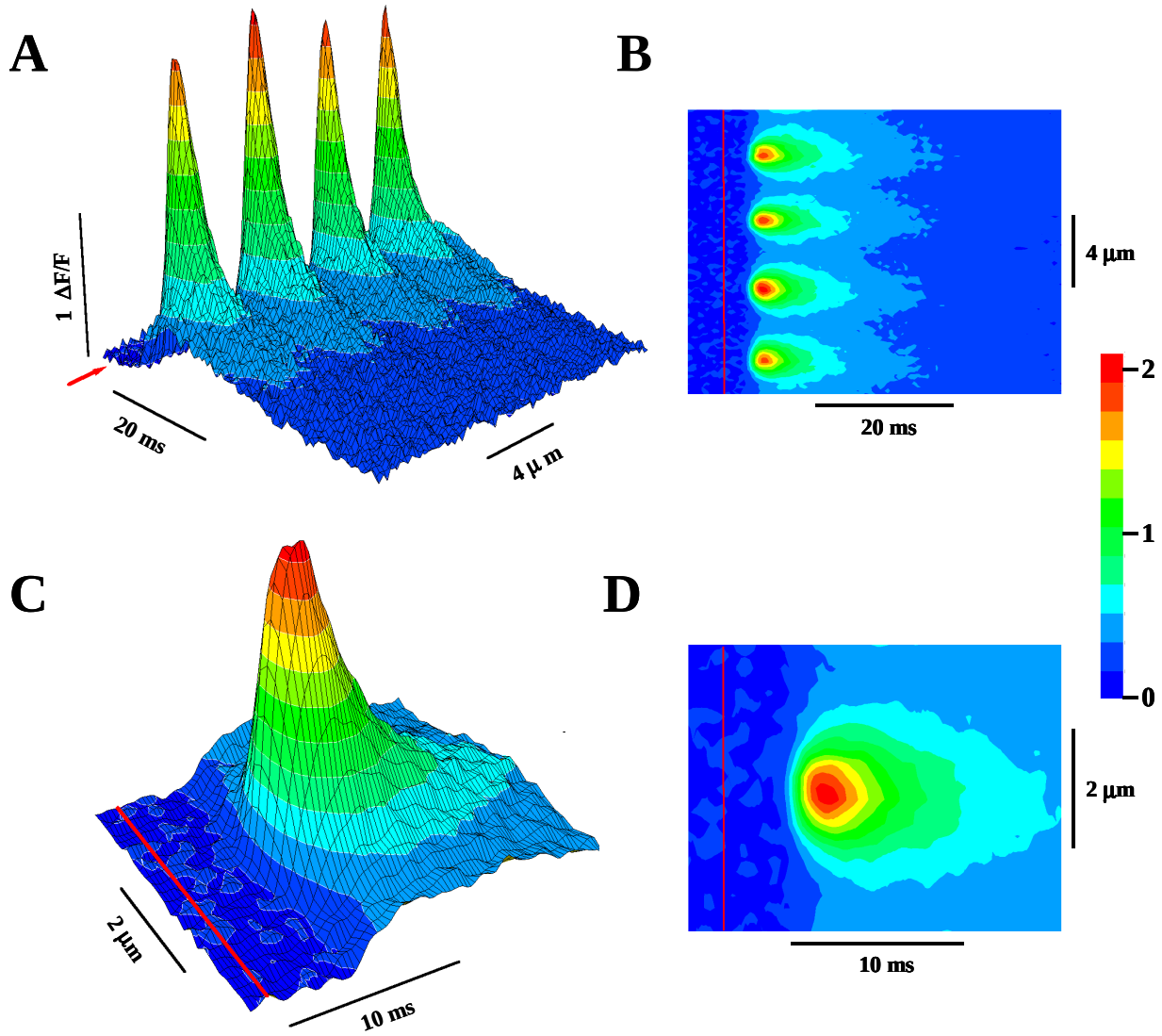


*Figure 4. $Ca^{2+}$-dependent OGB-5N fluorescence domains.* **A** and **B**: 3D and contour plots, respectively, of the $Ca^{2+}$-dependent OGB-5N fluorescence transients obtained by moving the muscle fiber across a distance of ~ 16 μm with a scanning step size of 200 nm. Panels A and B show the same 4 domains. **C** and **D**: Enlarged view of the central domain shown in panels A and B. The stimulus time is indicated by an *arrow* in A and by a *red line* in B through D. The calibration bar represents 12 color levels corresponding to ΔF/F values ranging from 0 to 2.2. Experimental conditions: [OGB-5N]: 500 μM, [EGTA]: 100 μM; sarcomere spacing: 4.4 μm; temperature: 17°C.

presynaptic $Ca^{2+}$ microdomains in a neuromuscular junction preparation has been recently accomplished using low affinity $Ca^{2+}$ indicators and the spot detection method[34]. Analogously, when AP-evoked OGB-5N ΔF/F transients are plotted as a function of distance (Figure 4), a clear portrait can be obtained of the topology of the inter- and intra-sarcomeric $Ca^{2+}$ dynamics. There are defined regions, regularly spaced along the muscle fiber, in which the $Ca^{2+}$ release originates and where the $[Ca^{2+}]$ changes are most pronounced. These regions, henceforth termed $Ca^{2+}$-release domains, are shown in Figures 4 in different perspectives: 3D plots in panels A and C, and contour maps in panels B and D. Figures 4A and 4B illustrate how the $Ca^{2+}$ domains originate in the region of the T-tubules for 4 consecutive sarcomeres and how they expand in time along the longitudinal axis of the fiber. The figure also provides evidence that the positional-dependence of the ΔF/F transients is preserved identically across several sarcomeres. The contour maps presented in Figures 4B and 4D demonstrate that every individual $Ca^{2+}$-release domain is centered symmetrically on the Z-line and that the onset of the ΔF/F transient at the M-line is slightly delayed with respect to the Z-line. The regular pattern of the 4 $Ca^{2+}$ domains shown in Figure 4A, and the bilateral symmetry of each of them (Figures 4B and 4D), demonstrate the intrinsic symmetry of the $Ca^{2+}$ release regions of the SR with respect to the Z-line. Furthermore, these results prove that, during an x-axis scan, the laser intensity required to obtain each AP-evoked transient did not affect the record obtained from the adjacent position (separated by 200 nm). In other words, the intensity of the excitation light was low enough as to not induce significant photodamage to the fiber. However, this was not always the case and in some occasions domains were skewed in the direction of the scan; these results were discarded.

An important aspect of the overall process of $Ca^{2+}$ release in skeletal muscle fibers that becomes patent in Figure 4 is the heterogeneous (yet stereotypical) $Ca^{2+}$ distribution in the myoplasm that persist for ~30 ms after AP stimulation. After this time, although the $[Ca^{2+}]$ gradients progressively dissipate, the $[Ca^{2+}]$ remains elevated throughout each sarcomere for another ~40 ms (Figure 4B). Figures 4C and 4D show expanded renditions of the central domain in Figures 4A and 4B to depict in more detail the formation of the $Ca^{2+}$ domain. It can be observed that the domain becomes first visible ~3 ms after the onset of the AP as a narrow region of increased ΔF/F which widens in time, reaching at its peak a FWHM of ~1.4 μm.

The spatiotemporal properties of $Ca^{2+}$-release domains give valuable information about features of the physiological $Ca^{2+}$ release process, such as the extent and localization of the $Ca^{2+}$ sources along the muscle fiber, and the diffusion of $Ca^{2+}$ throughout the sarcomeres. We will focus now on the quantitative evaluation of the size and rate of expansion of the domains in order to assess some of these properties. To this end, the domains' isochronal cross sections were fit to Gaussian curves in order to yield their FWHM[34]. A plot of isochronal sections obtained at 5 different times after stimulation during the rising phase of a $Ca^{2+}$ domain are shown in Figure 5A. It can be observed that during the 2.4 ms rising phase, the $Ca^{2+}$ domain grows in amplitude from a ΔF/F of 0.3 to 3, and in width, from a FWHM of 0.85 μm to 1.27 μm. Figure 5B shows another sequence of isochronal sections of the same domain, but in this case taken during its falling phase, that demonstrates the gradient dissipation from a $(\Delta F/F)_{peak}$ of ~1.9 to ~0.9 with an associated widening from 1.27 to 1.44 μm. As

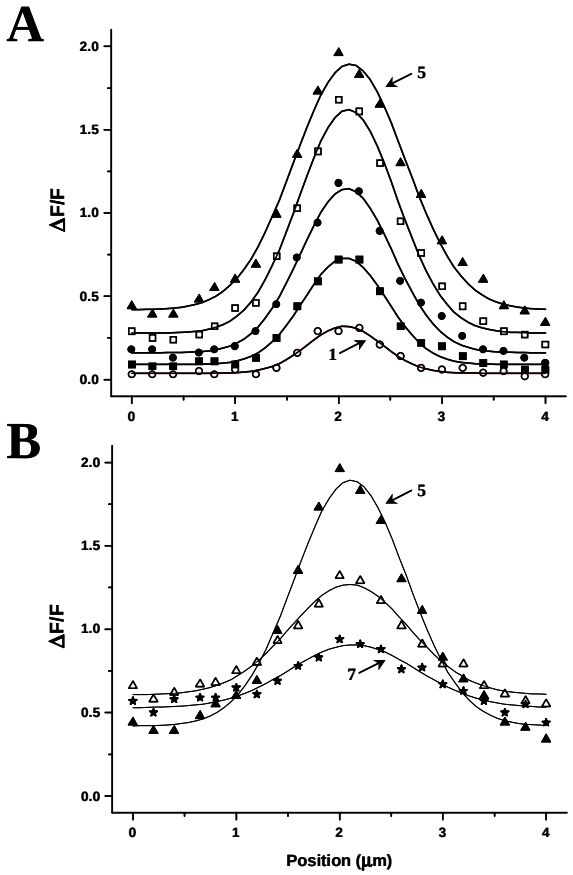


*Figure 5. Dimensions of a $Ca^{2+}$-release domain.* **A**: Isochronal ΔF/F plots of a single domain obtained at 5 different times after stimulation, from 3.4 ms (trace 1) to 5.8 ms, corresponding the peak time at the Z-line (trace 5). The FWHM of Gaussian curves fitted to the isochronal data (continuous lines) measured 0.85, 0.95, 1.05, 1.11 and 1.27 μm for traces 1 to 5, respectively. **B**: Isochronal plots of the same domain in A, obtained at 2 times after the peak (trace 5). Trace 7 was obtained 11 ms after stimulation. The FWHM of Gaussian curves fitted to the isochronal data (continuous lines) measured 1.27, 1.36, and 1.44 μm, for traces 5 to 7, respectively. Experimental conditions: [OGB-5N]: 500 μM, [EGTA]: 0.5 mM; sarcomere spacing: 4 μm; temperature: 18°C.

expected, all the isochronal spatial profiles are centered and symmetrical about the same position in the sarcomere (Z-line). At 18 °C the peak of the $Ca^{2+}$-release domains occurred 5.4 ± 0.8 ms (n = 38) after the AP stimulation, and 2.52 ± 0.5 ms after the initiation of the transient. At this point the FWHM was 1.4 ± 0.2 μm (n = 28). Obviously, this value of FWHM does not directly reflect on the actual size of the $Ca^{2+}$ release since that isochronal measurement was made at a time that allowed for diffusional expansion of the domain. Using an approach analogous to the characterization of $Ca^{2+}$ entry sites in presynaptic terminals[34], we could estimate the size of the $Ca^{2+}$ source by measuring the FWHM of the domain at the earliest time that it was detectable. We found for the data in Figure 5 that the expansion of the domain evolved at two different rates: a fast initial process, that occurs between the onset of the $Ca^{2+}$ release and the point at which the Z-line transient peaks (~4.8 ms), with an expansion rate of 0.15 μm/ms, and a significantly slower process of steady expansion (during which the $Ca^{2+}$ gradients dissipate) whose approximated rate is 0.02 μm/ms. Following the same approach, in 10 domains in 5 different fibers, the first isochronal cross section that was visible above the noise in fibers perfused with 500 μM OGB-5N and 0.5 mM EGTA at ~18 °C, occurred at 3.24 ± 0.56 ms (mean ± SD). Remarkably, the mean FWHM of the earliest detectable isochronal cross sections was 0.77 ± 0.25 μm. This value is significantly larger than the optical resolution of our optical system as determined by fluorescent bead calibrations and from the FWHM of di-8-ANEPPS labeled T-tubules (Figure 2).

## 4. DISCUSSION AND CONCLUSIONS

We have described the use of a stage scanning confocal microscope to measure AP-induced intrasarcomeric $Ca^{2+}$ transients in amphibian skeletal muscle fibers under physiological conditions. Using this optical setup, we obtained a detailed spatiotemporal portrait of the intrasarcomeric $Ca^{2+}$ movements that occur in response to an AP, which will allow us to initiate the quantitative assessment of processes that underlie $Ca^{2+}$ release in physiological E-C coupling.

The combination of a low capacitance PIN photodiode and a low noise integrating amplifier made it possible to measure fluorescence changes with a high signal-to-noise (s/n) ratio from a confocal detection volume as small as 0.3 μm diameter in the x-y plane and 0.75 μm in the x-z plane. This high spatial resolution and the use of nanopositioning actuators allowed us to discriminate time-dependent variations in the $[Ca^{2+}]$ from positions separated by 100-200 nm. These are significant improvements over the system described previously[12]. What makes the current confocal detection method ideal for studying AP-evoked $Ca^{2+}$ release in skeletal muscle fibers is not only its space resolution, which is comparable to other confocal microscopes, but its extremely low noise and the ability to acquire data at up to 50 kHz.

Our confidence in the spatial resolution of the spot detection system, based on extensive *in vitro* bead calibration experiments, was confirmed *in vivo* by staining of the T-tubules with the potentiometric indicator di-8-ANEPPS[10,28]. In this regard, an interesting result was that the FWHM of stained T-tubules, which are known to measure <100 nm in diameter, was significantly larger (0.49 ± 0.08 μm) than that of corresponding fluorescent beads of the same size (~0.3 μm). Part of this discrepancy could be due to the tortuous geometry of the T-system, which makes it very unlikely to have a single T-tubule within the detection volume of our system. In fact, high magnification electron micrographs of frog skeletal muscle fibers show that the T-tubules wander around the Z-line in an arbitrary manner[4,11,29,30]. It could also be due to the fact that the fiber represents an anisotropic and complex optical media, which could alter the point spread function of the microscope. Nevertheless, a sucrose-agar solution designed to mimic the refractive index of the fiber had no effect on the spatial resolution as determined by in vitro bead calibrations (data not shown).

Although 4 μm is not the physiological slack sarcomere length of frog skeletal muscle fibers, stretching doesn't seem to affect significantly the $Ca^{2+}$ release process, as evidenced by the large $(\Delta F/F)_{peak}$ values obtained with OGB-5N at the Z-lines. On the contrary, our results indicate a robust $Ca^{2+}$ release, leading to peak $[Ca^{2+}]$ changes of ~9 μM at the Z-line, and, surprisingly, ~ 2 μM at the M-line. Besides not having deleterious effects, stretching affords several advantages for our experimental approach. Firstly, separating simultaneously activated adjacent sources of $Ca^{2+}$ release afforded us a larger number of spot positions sampled with our finite probe. Thus, increasing the sarcomere length was equivalent to increasing the lateral spatial resolution of the detection system, and allowed for a more detailed description of intrasarcomeric $Ca^{2+}$ movements. In addition, increasing the distance between the Z- and M-lines, favors the detection of Z-M delays. Finally, separating $Ca^{2+}$ sources minimizes the effect that adjacent sources have on each other. In other words, the $Ca^{2+}$ release domains described in this work closely represent the contribution of individual $Ca^{2+}$ release sites to the $[Ca^{2+}]$ profiles along the sarcomere, with only small effects arising from neighboring sites.

The characterization of $Ca^{2+}$ release domains using the confocal spot detection technique and the sampling protocol described in this work was only possible since the $Ca^{2+}$ release is a stereotyped process, both in time and space. Thus, following each AP stimulation, the release of $Ca^{2+}$ ions from the SR was repeated identically throughout the muscle fiber. Although, at the global detection level, this repeatability had been well documented previously[25], our work shows, for the first time, that there is a high similarity between $Ca^{2+}$ signals recorded at equivalent positions of the sarcomere for different $Ca^{2+}$ release sites (Figure 4). This result indicates that the structures underlying a $Ca^{2+}$ release domain at each triad are

extraordinarily similar to each other, and that the activation of the E-C coupling by an AP proceeds in a highly repeatable fashion. Our work also shows for the first time, that at every particular sarcomere location, there is a reproducible $Ca^{2+}$ release process in response to every AP. This can be readily inferred from the characteristic bilateral symmetry and periodic distribution of the kinetic parameters for fluorescence transients recorded along a sarcomere. Any significant fluctuation in the $Ca^{2+}$ release in response to consecutive stimulations would have resulted in a random pattern.

After the introduction of localized detection methods to study E-C coupling in skeletal muscle[12] subsequent confocal fluorescence studies have been performed primarily using beam scanning (BS) confocal microscopes to investigate the spatiotemporal properties of spontaneous $Ca^{2+}$ release events ($Ca^{2+}$ sparks). The sparks are localized $Ca^{2+}$ release events, which have been proposed to represent elementary processes underlying $Ca^{2+}$ release during E-C coupling[35,36]. In contrast, in this study we focus on the measurement of localized $Ca^{2+}$ domains evoked by the physiological activation of the $Ca^{2+}$ release mechanisms by an AP. As such, our work provides valuable reference data challenging the putative physiological role of the $Ca^{2+}$ sparks since both phenomena have been studied with comparable spatial resolution. The comparison between the spatiotemporal properties of $Ca^{2+}$ sparks and our $Ca^{2+}$ domains suggests that if sparks truly represent elementary events in skeletal muscle E-C coupling, their stochastic recruitment to yield an evoked physiological response must be exquisitely synchronized.

In 1994, our laboratory reported that the onset of AP-evoked $Ca^{2+}$-dependent fluorescence signals recorded from skeletal muscle fibers at the M-line was not significantly delayed with respect to those at the Z-line[12]. Although in a subsequent publication[13] we noticed that deblurred pulsed laser images of $Ca^{2+}$ gradients recorded early after AP stimulation showed some delay between M-line and Z-line fluorescence, and later confirmed the existence of a Z-M delay by improving the confocality of the spot detection system[14], the issue has remained debatable ever since. Recently, Hollingworth *et al.*[15] measured localized AP-evoked $Ca^{2+}$ transients using a BS microscope in intact frog skeletal muscle fibers injected with Fluo-3 and reported the existence of ~1 ms Z-M delay at 22 $^{o}$C. In this paper we very carefully examined the kinetic properties of Z- and M-line transients using a confocal detection system with a resolution comparable (or slightly better) than these authors', a low affinity $Ca^{2+}$ indicator with an improved kinetic response with respect to Fluo-3[37], and stretched muscle fibers to sarcomere spacings of ~4 μm. Moreover, we used a very stringent criterion to determine the onset time of the fluorescence transients (3 S.D. above baseline, see Methods). Under these conditions, we found Z-M delays to be detectable, but very short (0.86 ± 0.42 ms at ~18 $^{o}$C, $p<0.001$). If the increase in dye fluorescence along the sarcomere is visualized as a wavefront advancing from the Z-line towards the M-line, its speed of propagation would be ~2.3 μm/ms. This value is at least an order of magnitude larger than the speed of propagation of $Ca^{2+}$ waves (typically in the tens of μm/s) recorded in other biological preparations[38,39]. Moreover, a myofibril model of $Ca^{2+}$ diffusion in the sarcomere in which an infinitesimal release site is located at the Z-line, and which includes realistic kinetic binding parameters to myoplasmic proteins, predicts a Z-M delay of at least 3 ms for a half-sarcomere distance of 2 μm[40]. According to Hollingworth *et al.*[15], the inclusion of mobile $Ca^{2+}$ buffers in the model and corrections for distortions due to dye binding to intracellular proteins and misregistration between sarcomeres, leads to predicted Z-M delays of ~1 ms for a half-sarcomere distance of 1.6 μm. Nevertheless, this value is still too large to explain ours, considering the larger sarcomere spacing in our measurements. Moreover, we independently demonstrated, from T-tubule staining experiments, that under our experimental conditions the upper limit for the uncertainty in the location of the release sites is 0.49 μm, and we have never observed the severe phase shifts along longitudinal scans that prompted these authors to introduce misregistration corrections. An alternative explanation to account for the short Z-M delays observed experimentally is to assume that a relatively broad band of $Ca^{2+}$ release sites (probably spanning both terminal cisternae of the triad) is rapidly engaged after the AP activation[12]. There are two lines of evidence in support of this possibility. Firstly, the presence of extra-junctional RyR $Ca^{2+}$ release channels has been demonstrated in the membranes of skeletal muscle SR[41]. Secondly, the surprising results obtained here indicating that the smallest detectable isochronal cross section of $Ca^{2+}$ domains has a FWHM of ~0.8 μm. This result cannot be readily explained by limitations in the axial resolution of the detection system since fluorescently stained T-tubules reported significantly narrower FWHM of ~0.5 μm. Moreover, our bead calibration experiments demonstrated that the detection system in the x-axis is linearly accurate for objects of dimensions larger than 0.5 μm. It could be argued that the low affinity of OGB-5N might contribute to the large size of the earliest detectable width of the $Ca^{2+}$ domain since it could miss relatively small [$Ca^{2+}$] changes occurring early after AP stimulation. However, we have performed control experiments using the high affinity indicator OGB-2[26] and found results similar to those with OGB-5N (data not shown). We are currently investigating the role of mechanisms that might be responsible for the existence of a relatively wide band of $Ca^{2+}$ release. We developed a 3D model of the sarcomere that includes localized or delocalized sources of $Ca^{2+}$ and takes into account the limitations of our optical detection system, which will be used to test this hypothesis[42]. Also, since the most likely candidate for the recruitment of extrajunctional RyR channels might be a $Ca^{2+}$-induced-$Ca^{2+}$-release mechanism, we are studying the effects of caffeine on localized $Ca^{2+}$ domains[43].

## ACKNOWLEDGEMENTS

This work was supported by the National Institutes of Health/National Institute of Arthritis and Musculoskeletal and Skin Diseases (NIAMS) grant AR-25201.

## REFERENCES

1. Huxley, A. F. & Taylor, R. E. "Local activation of striated muscle fibers", *J. Physiol.* **144**, pp. 426-451, 1958.
2. Sandow, A. "Excitation-contraction coupling in skeletal muscle", *Pharmacol. Rev.* **17**, pp. 265-320, 1965.
3. Podolsky, R. J., Hall, T. & Hatchett, S. L. "Identification of oxalate precipitates in striated muscle fibers", *J. Cell Biol.* **44**, pp. 699-702, 1970.
4. Peachey, L. D. "The sarcoplasmic reticulum and transverse tubules of the frog's sartorius", *Journal of Cell Biology* **25**, pp. 209-231, 1965.
5. Tanabe, T., Beam, K. G., Adams, B. A., Niidome, T. & Numa, S. "Regions of the skeletal muscle dihydropyridine receptor critical for excitation-contraction coupling", *Nature* **346**, pp. 567-9, 1990.
6. Rios, E., Ma, J. J. & Gonzalez, A. "The mechanical hypothesis of excitation-contraction", *J. Muscle Res. and Cell Mot.* **12**, pp. 127-35, 1991.
7. Adrian, R. H., Chandler, W. K. & Hodgkin, A. L. "The kinetics of mechanical activation in frog muscle", *J. Physiol.* **204**, pp. 207-30, 1969.
8. Adrian, R. H. & Peachey, L. D. "Reconstruction of the action potential of frog sartorius muscle", *J. Physiol.* **235**, pp. 103-31, 1973.
9. Vergara, J. & Bezanilla, F. "Fluorescence changes during electrical activity in frog muscle stained with merocyanine", *Nature* **259**, pp. 684-6, 1976.
10. Kim, A. M. & Vergara, J. L. "Supercharging accelerates T-tubule membrane potential changes in voltage clamped frog skeletal muscle fibers", *Biophys. J.* **75**, pp. 2098-116, 1998.
11. Zampighi, G., Vergara, J. & Ramon, F. "On the connection between the transverse tubules and the plasma membrane in frog semitendinosus skeletal muscle. Are caveolae the mouths of the transverse tubule system?", *J. Cell Biol.* **64**, pp. 734-40, 1975.
12. Escobar, A. L., Monck, J. R., Fernandez, J. M. & Vergara, J. L. "Localization of the site of Ca2+ release at the level of a single sarcomere in skeletal muscle fibres", *Nature* **367**, pp. 739-41, 1994.
13. Monck, J. R., Robinson, I. M., Escobar, A. L., Vergara, J. L. & Fernandez, J. M. "Pulsed laser imaging of rapid Ca2+ gradients in excitable cells", *Biophys. J.* **67**, pp. 505-14, 1994.
14. Escobar, A. L., Vergara, J. L., Fernandez, J. & Monck, J. "Excitation-contraction coupling in single sarcomeres of frog skeletal muscle fibres", *J. Muscle Res. and Cell Mot.* **17**, pp. 375, 1996.
15. Hollingworth, S., Soeller, C., Baylor, S. M. & Cannell, M. B. "Sarcomeric Ca2+ gradients during activation of frog skeletal muscle fibres imaged with confocal and two-photon microscopy", *J. Physiol.* **526**, pp. 551-60, 2000.
16. Endo, M., Tanaka, M. & Ogawa, Y. "Calcium induced release of calcium from the sarcoplasmic reticulum of skinned skeletal muscle fibres", *Nature* **228**, pp. 34-6, 1970.
17. Ford, L. E. & Podolsky, R. J. "Regenerative calcium release within muscle cells", *Science* **167**, pp. 58-9, 1970.
18. Fabiato, A. & Fabiato, F. "Contractions induced by a calcium-triggered release of calcium from the sarcoplasmic reticulum of single skinned cardiac cells", *J. Physiol.* **249**, pp. 469-95, 1975.
19. DiFranco, M., Novo, D. & Vergara, J. L. "Characterization of the Calcium Release Domains during Excitation-Contraction Coupling in Skeletal Muscle Fibres", *(submitted)*, pp. , 2001.
20. Castleman, K. *Digital Image Processing* Prentice Hall, New York, 1979.
21. Wilson, T. *Confocal Microscopy* Academic Press, New York, 1990.
22. DiFranco, M. *et al.* "Inverted double-gap isolation chamber for high-resolution calcium fluorimetry in skeletal muscle fibers", *Pflugers Arch* **438**, pp. 412-8, 1999.
23. Huxley, A. F. & Niedergerke, R. "Measurement of the striations of isolated muscle fibres with the interference microscope", *Journal of Physiology* **144**, pp. 403-425, 1958.
24. Vergara, J., Bezanilla, F. & Salzberg, B. M. "Nile blue fluorescence signals from cut single muscle fibers under voltage or current clamp conditions", *Journal of General Physiology* **72**, pp. 775-800, 1978.
25. Vergara, J. & DiFranco, M. "Imaging of calcium transients during excitation-contraction coupling in skeletal muscle fibers", *Adv Exp Med Biol* **311**, pp. 227-36, 1992.

26. DiGregorio, D. A. & Vergara, J. L. "Localized detection of action potential-induced presynaptic calcium transients at a Xenopus neuromuscular junction", *J Physiol (Lond)* **505**, pp. 585-92, 1997.
27. Lopez, J. R., Alamo, L., Caputo, C., DiPolo, R. & Vergara, J. L. "Determination of ionic calcium in frog skeletal muscle fibers", *Biophys J* **43**, pp. 1-4, 1983.
28. Kim, A. M. & Vergara, J. L. "Fast voltage gating of Ca2+ release in frog skeletal muscle revealed by supercharging pulses", *J Physiol (Lond)* **511**, pp. 509-18, 1998.
29. Peachey, L. D. "Transverse tubules in excitation-contraction coupling", *Fed. Proc.* **24**, pp. 1124-34, 1965.
30. Franzini-Armstrong, C. "Studies of the triad. 3. Structure of the junction in fast twitch fibers", *Tissue and Cell* **4**, pp. 469-78, 1972.
31. Brakenhoff, G. J., Van Spronsen, A., Van der Voort, H. T. M. & Nanninga , N. "Three-dimensional confocal fluorescence microscopy", *Methods in Cell Biology* **30**, pp. 379-398, 1989.
32. Chad, J. E. & Eckert, R. "Calcium domains associated with individual channels can account for anomalous voltage relations of Ca-dependent responses", *Biophysical Journal* **45**, pp. 993-9, 1984.
33. Augustine, G. J., Charlton, M. P. & Smith, S. J. "Calcium action in synaptic transmitter release", *Annual Review of Neuroscience* **10**, pp. 633-93, 1987.
34. DiGregorio, D. A., Peskoff, A. & Vergara, J. L. "Measurement of action potential-induced presynaptic calcium domains at a cultured neuromuscular junction", *Journal of Neurosciences* **19**, pp. 7846-59, 1999.
35. Tsugorka, A., Rios, E. & Blatter, L. A. "Imaging elementary events of calcium release in skeletal muscle cells", *Science* **269**, pp. 1723-6, 1995.
36. Klein, M. G. *et al.* "Two mechanisms of quantized calcium release in skeletal muscle", *Nature* **379**, pp. 455-8, 1996.
37. Escobar, A. L. *et al.* "Kinetic properties of calcium indicators: rapid transient responses to flash photolysis of DM-nitrophen.", *Pflugers Archiv* **434**, pp. 615-631, 1997.
38. Blatter, L. A. & Wier, W. G. "Agonist-induced [Ca2+]i waves and Ca", *American Journal of Physiology* **263**, pp. H576-86, 1992.
39. Girard, S. & Clapham, D. "Acceleration of intracellular calcium waves in Xenopus oocytes by calcium influx", *Science* **260**, pp. 229-32, 1993.
40. Cannell, B. M. & Allen, D. G. "Model of calcium movements during activation in the sarcomere of the frog skeletal muscle", *Biophysical Journal* **45**, pp. 913-925, 1984.
41. Dulhunty, A. F., Junankar, P. R. & Stanhope, C. "Extra-junctional ryanodine receptors in the terminal cisternae of mammalian skeletal muscle fibres", *Proceedings of the Royal Society of London. Series B: Biological Sciences* **247**, pp. 69-75, 1992.
42. Novo, D., DiFranco, M. & Vergara, J. L. "A 3-D cylindrical diffusion-reaction model of a single myofibril to study localized calcium signaling in skeletal muscle", *Proceeding of The Biophysical Society Meeting, Boston, MA*, 2001.
43. Vergara, J. L., DiFranco, M. & Novo, D. "Confocal study of the effects of caffeine on calcium release elicited by action potential stimulation", *Proceeding of the Biophysical Society Meeting, Boston, MA*, 2001.